4. Forming

This text corresponds to e-book "Introduction to the Principles of Ceramic Forming", ISBN 3-87264-016-X [4].

4.1 Introduction

With the exception of some new developments nearly all ceramic forming processes may be classified by three groups, i.e. „casting“, „plastic forming“ or „pressing“.

In such processes the starting powders are prepared in aqueous or organic solvents in the beginning. In case of casting these suspensions are directly processed while plastic forming requires partly dewatered feeds and almost completely dry granules are used in the pressing process.

To produce stable suspensions both the surface condition of the powder particles and the interaction with the suspension media are of utmost importance. That is why the first chapter deals with general principles on this subject and describes the plasticity of ceramic systems and the production of granules from suspensions.

In the second part the individual forming processes will be discussed, laying special stress on theoretic principles. Chapter two closes with the description of some new developments whose suitability in practical applications is still pending to some extent. Not everyone looking for practical help in this introduction will find it. May be this paper serves only as basic information for engineers to continue elaborating their own solutions for special problems that may arise in practical application.

4.2 General principles

In almost all forming processes applied for manufacturing ceramic products basically powders are dispersed, mixed and homogenized in water or organic solvents. For the further treatment of these suspensions it is essential to understand the reactions at the surface of the powder particles.

4.2.1 Characterisation of suspensions

4.2.1.1 Particle charging in liquid suspensions

Ceramic powders normally have a high specific surface to show electric charges in aqueous suspensions. Such electric charges may be explained as follows: oxides show unsaturation at their surface due to the incomplete coordination of atoms. When these oxide surfaces get in contact with water the surface becomes hydrated [1].

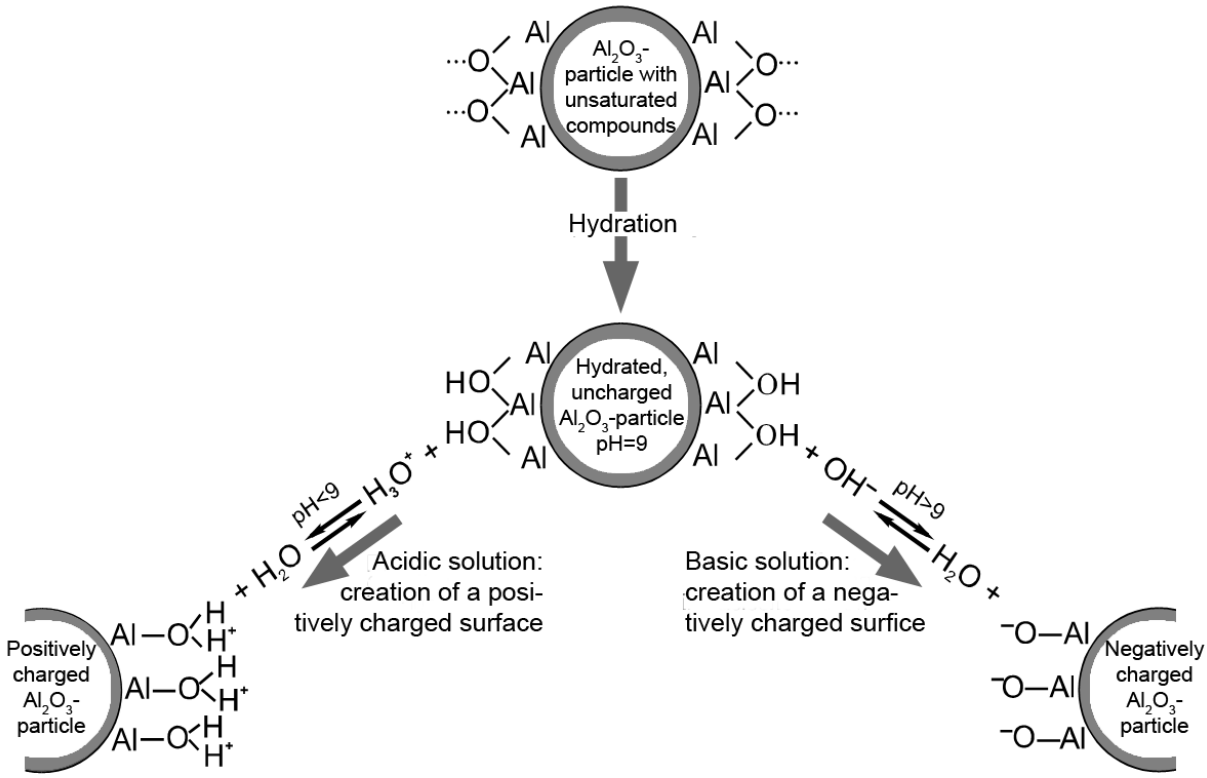

Fig. 4.2.1.1.1: Creation of a hydrated Al_20_3 particle surface and their reaction in acidic and basic solutions (schematic).

In this process protons from the liquid phase are added to surface oxygen ions and create a neutral particle with OH groups at the surface. The surface charges are created subject to the pH of the suspension either by absorbing H^+ or OH^- ions or by dissociating the surface charged OH groups. This mechanism can be seen from fig. 4.2.1.1.1.

The processes appearing at the hydrated surface of an oxide are therefore determined by the chemical reactions

$$MeOH_{(surface)} + H_3O^+_{(solution)} \xleftrightarrow{K_1} MeOH_2^+{}_{(surface)} + H_2O$$

$$MeOH_{(surface)} + OH^-_{(solution)} \xleftrightarrow{K_2} MeO^-_{(surface)} + H_2O,$$

where Me is a metal ion at the surface, i.e. Ba^{2+}, Al^{3+} or Si^{4+}. By adding H_3O^+ ions the pH will be reduced as the uncharged surface absorbs protons and thus becomes positively charged. The addition of OH^- ions separates hydrogen from the surface and produces a negative surface charge with pH values that are higher than the point of zero charge (PZC) at the surface.

The point of zero charge – frequently also called isoelectric point (IEP) – of the surface reflecting the acid-base character is given by the two pKs of the above reactions [2].

$$PZC = \frac{pK_1 + pK_2}{2}.$$

According to the valence of the cation and the coordination of the oxygen ions the number of surface charges will vary and the point of zero charge will be shifted.

For pure aluminium oxide the PZC lies at pH= 9. For other oxides with varying crystalline structures the pH values for the point of zero charge will be different (Fig. 4.2.1.1.2).

The creation of surface charges in layer minerals like kaolinite has other reasons. In the tetrahedral di-silicate layer four-valence silicon ions may be replaced by trivalent aluminium ions, in the octahedral gibbsite layer aluminium ions may be replaced by bivalent magnesium ions or by other ions of equal valence by incorporating alkali or earth alkali ions into the lattice for valence compensation. In case of incomplete valence compensation charges will appear at the surface of the kaolinite particles. Moreover, the relatively dissolute alkali or earth alkali ions that are incorporated in the intermediate layers of the kaolinite structures may be absorbed in aqueous media and create additional negative surface charges (Fig. 4.2.1.1.3).

Material	Chemical composition	IEP
Muscovite	$KAl_3Si_3O_{11}·H_2O$	1
Quartz	SiO_2	2
δ-Manganese oxide	MnO_2	2
Soda lime silica glass	1,00 Na_2O·0,58 CaO·3,70 SiO_2	2-3
Albite	$Na_2O·Al_2O_3·6\ SiO_2$	2
Orthoclase	$K_2O·Al_2O_3·6\ SiO_2$	3-5
Silica (amorphous)	SiO_2	3-4
Zirconia	ZrO_2	4-5
Rutile	TiO_2	4-5
Tin oxide	SnO_2	4-7
Apatite	10 CaO·6 PO_2·2 H_2O	4-6
Zircon	$SiO_2·ZrO_2$	5-6
Anatase	TiO_2	6
Magnetite	Fe_3O_4	6-7
Haematite	α-Fe_2O_3	6-9
Goethite	FeOOH	6-7
γ-Iron oxide	γ-Fe2O3	6-7
Kaolin (edges)	$Al_2O_3·SiO_2·2\ H_2O$	6-7
Chromium oxide	α-Cr_2O_3	6-7
Mullite	3 Al_2O_3·2 SiO_2	7-8
γ-Alumina	γ-Al_2O_3	7-9
α-Alumina	α -Al_2O_3	9-9,5
Alumina (Bayer process)	Al_2O_3	7-9,5
Zinc oxide	ZnO2	9
Copper oxide	CuO	9
Barium carbonate	$BaCO_3$	10-11
Yttria	Y_2O_3	11
Lanthanum oxide	La_2O_3	10-12
Silver oxide	Ag_2O	11-12
Magnesa	MgO	12-13

Fig. 4.2.1.1.2: Point of zero charge (IEP) of different oxides in watery suspensions [2].

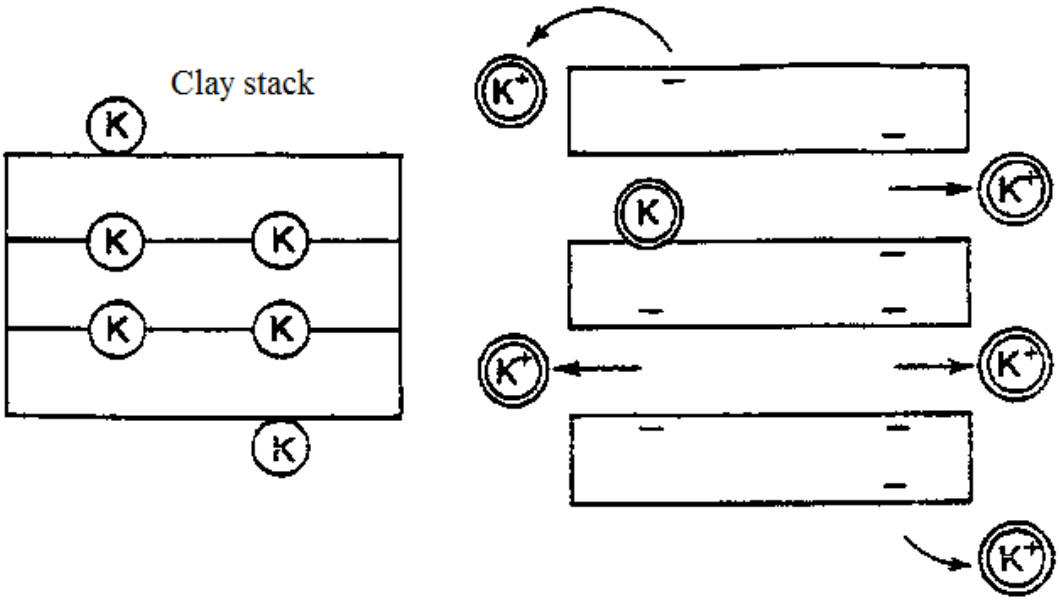

Fig. 4.2.1.1.3: Formation of surface charges at clay stacks by liberating alkali ions from the intermediate layers (schematic) [2].

Apart from the cation exchange capacity there is also an anion exchange capacity available at the edges of the kaolin particles that give rise to positively charged surfaces. This was made visible in an electron-microscope by Thiessen [3] upon the adsorption of negatively charged colloidal gold particles (Fig. 4.2.1.1.4).

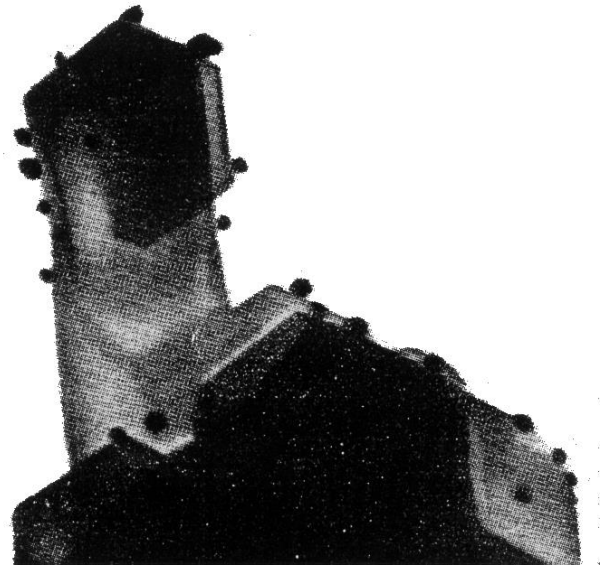

Fig. 4.2.1.1.4: Adsorption of a negatively charged gold colloid on kaolin particles [3].

4.2.1.2 Electrical double layers on particle surfaces

In ceramic slurries particles with charged surfaces are surrounded by ions and polar molecules. Equally charged ions are repulsed due to the Coulomb force while oppositely charged ions and polar molecules are attracted. That is why the concentration of counter ions increases at the particle surface and an electric potential is created between the surface and the suspension (Fig. 4.2.1.2.1).

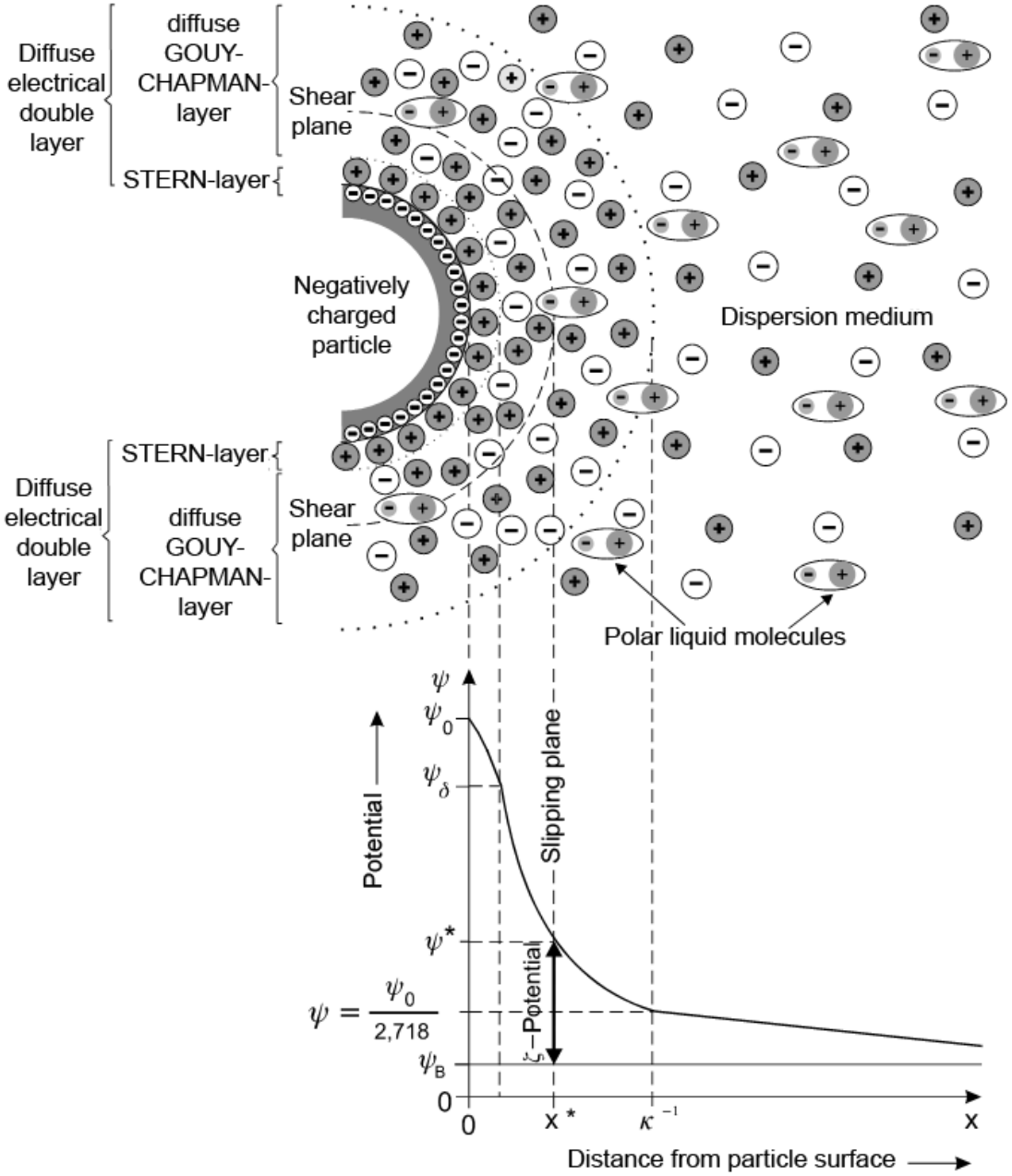

Fig. 4.2.1.2.1: Diffuse electric double layer at a solid particle surface in aqueous suspension and potential gradient between particle surface and suspension (schematic).

At the interface between powder particles and dispersion medium the solid particles are surrounded by a layer of absorbed ions that fit relatively tight to the particle surface. Helmholtz [4] implied that every negative charge of the particle was saturated by a counter ion, but for steric reasons the counter ions will not, as a rule. That is why in the farer surroundings of the powder particles a so-called diffuse electric double layer is built up by a concentration gradient of counter ions and polar molecules of the liquid (fig. 4.2.1.2.1). The potential gradient is no sharp line, as a diffusion of counter ions will be caused by the thermic movement of molecules.

The built-up of this diffuse electrical double layer has been discussed and modified by Stern [5] as well as by Gouy [6] and by Chapman [7]. The potential gradient of the diffuse interfacial layer can be calculated accordingly both for a continuously charged surface and a solution with continuous dielectric constant ε_r and point charges. Assuming that the charge distribution can be described by the Boltzmann equation the result is the concentration of counter ions N_i in the diffuse layer compared to the concentration of ions in the solution N_i^0.

$$N_i = N_i^0 \exp\left(-\frac{U_i}{k_B T}\right).$$

The potential energy of the ions U_i is a function of the valence z_i of the ion, the electron charge e and the electric potential ψ at the respective position

$$U_i = z_i e \psi.$$

For a surface potential $\psi_0 \leq 100$ mV is

$$\psi = \psi_0 \exp(-\kappa x)$$

where x is the distance from the particle surface and the Debye constant

$$\kappa = \left(\frac{e^2 \sum N_i^0 z_i^2}{\varepsilon k_B T}\right)^{1/2}.$$

The surface potential thus decreases exponentially in the first approximation with the distance from the particle surface. When $x = \kappa^{-1}$ is $\psi = \psi_0/2{,}718$ (see fig. 4.2.1.2.1). From the ionic strength $I = \frac{1}{2} \Sigma c_i z_i^2$ (c_i = ionic concentration in mol/l) results the thickness of the diffuse electric double layer as

$$\kappa^{-1} = \left(\frac{2000 e^2 N_A I}{\varepsilon k_B T} \right)^{1/2} ,$$

where N_A is the Avogadro's number. For water of 25 °C a thickness of the diffuse electric double layer of 9,6 nm is calculated for a 0,001 molar 1:1 electrolytic solution according to Horn [8].

By modifying the concentration or the valence of the counter ions and by varying the dielectric constant ε_r and the temperature of the liquid the thickness of the diffuse electric double layer may be varied which is of decisive importance for the stabilization of ceramic slurries.

4.2.1.3 Electrokinetic properties and slip stability

In an electric field electrically charged particles move with a certain speed, the so-called electrophoretic velocity. A part of the diffuse electric double layer passes with the particles through the liquid. So a slippage plane is built up within the diffuse electric double layer to transport the surface ions or polar molecules through the liquid. In figure 4.2.1.2.1 ψ_0 is the potential of the particle surface, ψ_B the potential of the surrounding liquid, ψ_S the potential of the Stern layer and ψ^* the potential of the hypothetic slippage plane. The potential difference between the potential ψ^* of the slippage plane and the potential ψ_B of the surrounding liquid is called electrokinetic potential or zeta potential. The zeta potential can be calculated as follows according to Reed [2].

$$\varsigma = \frac{f_H \eta v_e}{\varepsilon_r \varepsilon_0 E} ,$$

where η is the viscosity of the electrolyte and v_e is the electrophoretic velocity for an imposed electric field E. The ratio v_e /E is the electrophoretic mobility.

The Henry constant f_H is equal to 1, when the product of the particle diameter d and the Debye constant κ is greater than 100 and 3/2 when d· κ is less than 1.

The size of the zeta potential depends on the thickness of the double layer D as well as on the total charge of the ions settled down on the particle surface. The addition of electrolyte to a slip of constant water content leads first to an increase in thickness of the double layer and to an increase of the total charge, i.e. the zeta potential grows.

When the double layer is at it‘s optimum the zeta potential will decrease again, as only the potential of the aqueous solution ψ_B will be increased (Fig. 4.2.1.2.1). This appearance is to be observed both at negatively and at positively charged particle surfaces. The pH with a zeta potential of 0 is called the isoelectric point (IEP). The schematic course of the zeta potential as a function of the pH is to be seen from fig. 4.2.1.3.1.

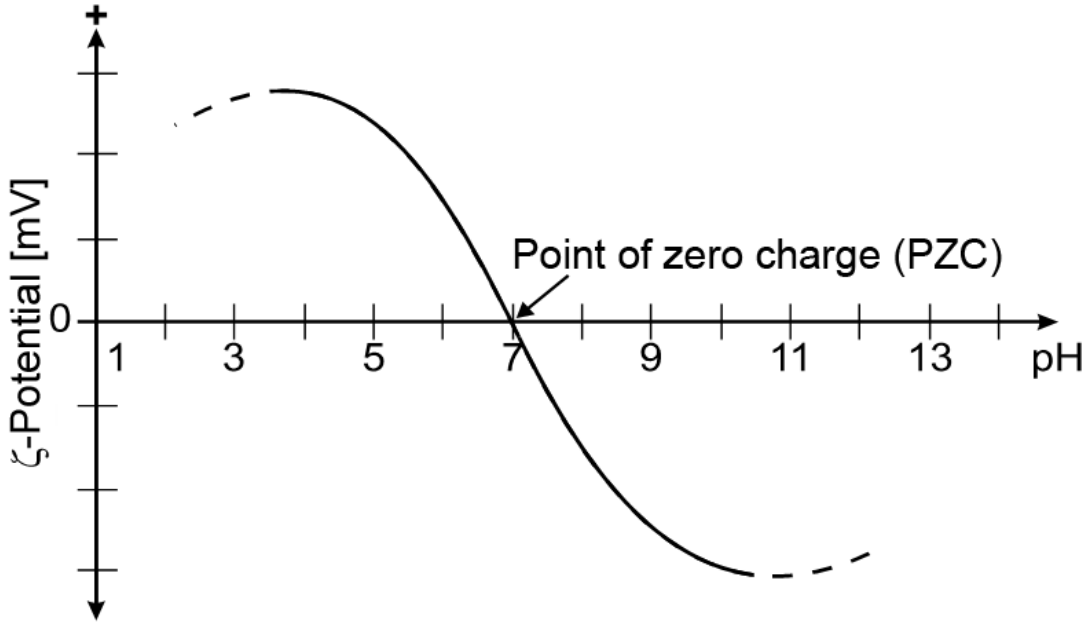

Fig. 4.2.1.3.1: Zeta potential as a function of the pH of the solution (schematic).
The increase of the zeta potential both at positively and negatively charged particle surfaces corresponds to the increase in thickness of the diffuse electric double layer.

The interaction of two particles with the same surface charge is described in the so-called DLVO theory both by Derjaguin and Landau [9] and by Verwey und Overbeek [10]. Van-der-Waals attractive forces are the driving force for the coagulation of the particles. For small particle diameters d and the distance of the particle surfaces h the potential energy for the attraction is obtained by the equation

$$U_{anziehend} = \frac{\left(\sqrt{A_2} - \sqrt{A_1}\right)^2 \cdot d}{24 \cdot h} \quad , \quad \textbf{attractive}$$

where A_1 and A_2 are the Hamaker constants for particles and dispersion medium.

In order to avoid an agglomeration repulsive forces have to react against the particle attraction. These repulsive forces may result from the interaction between electric double layers. They depend on the size and shape of the particles, the distance h between their surfaces, the thickness of the double layer κ^{-1} and the dielectric constant ε_r of the liquid medium. According to the Coulomb law the potential energy of the repulsive forces is calculated as follows for values of $d/\kappa^{-1} \ll 1$, i.e. for small particles with relatively large double layer

$$U_{abstoßend} = \frac{\varepsilon_r \cdot d^2 \cdot \psi_0^{\,2}}{4\left(h + d\right)} \cdot \exp\left(-\frac{h}{\kappa^{-1}}\right) \quad . \quad \textbf{repulsive}$$

When the particle diameter is much bigger than the electric double layer, as this is normally the case for ceramic powder particles in aqueous suspension, i.e. for $d/\kappa^{-1} \gg 1$, the following equation is applicable

$$U_{abstoßend} = \frac{\varepsilon_r \cdot d \cdot \psi_0^{\,2}}{4} \cdot \ln\left[1 + \exp\left(-\frac{h}{\kappa^{-1}}\right)\right] . \quad \textbf{repulsive}$$

The total potential energy is obtained from the sum of the attracting van-der-Waals potential energy and the repulsive potential energy as per

$$U_{total} = U_{attracting} + U_{repulsive}$$

If the attracting forces between the powder particles prevail in a suspension (Fig. 4.2.1.3.2), the particles will coagulate.

If the repulsive forces prevail because of the formation of electric double layers, suspensions may be stabilised as may be seen from Fig. 4.2.1.3.2.

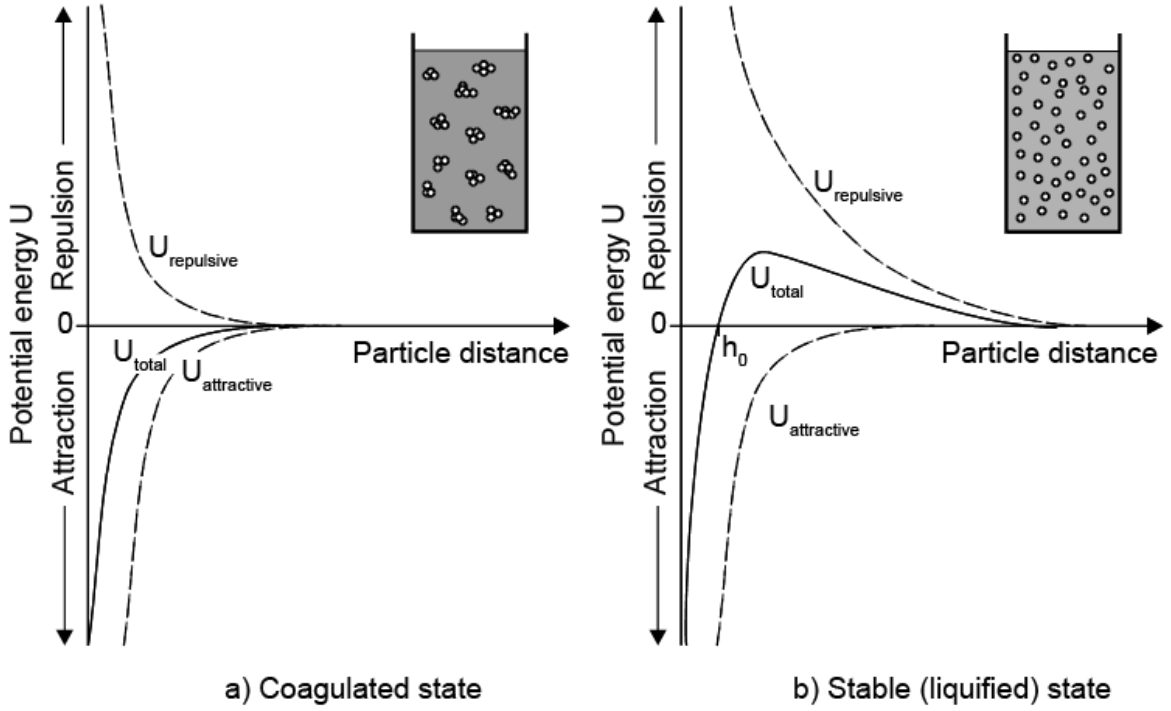

Fig. 4.2.1.3.2: Slip stability and potential energy as a result of the surface condition of particles in an aqueous suspension.

The addition of longer-chain molecules to a charged particle will moreover result in a steric hindrance of the approach of individual particles (Fig. 4.2.1.3.3).

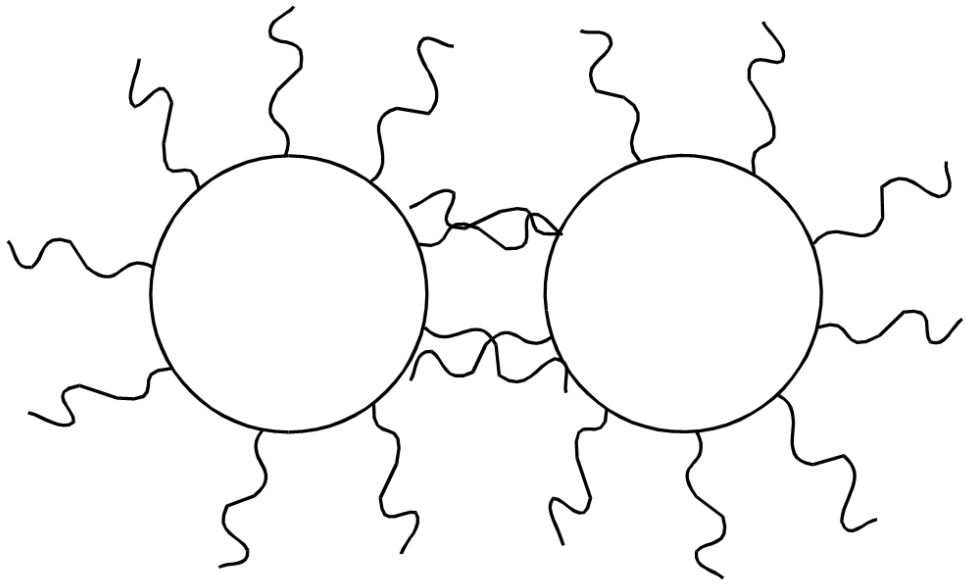

Fig. 4.2.1.3.3: Steric hindrance of the approach of powder particles in a suspension by long-chain molecules settled down (schematic).

The total repulsive potential energy is obtained then from

$$U_{total} = U_{attracting} + (U_{repulsive\ electrostatic} + U_{repulsive\ steric})$$

The steric repulsion is proportional to the thickness of the adsorbed layer and to the chemical composition respectively the concentration of the adsorbed molecules. A particle surface with long-chain molecules settled down on it will avoid the direct interaction between two neighbour particles especially when the surface charges are partly screened by the polymer chains so that the ion concentration around the particles decreases. This corresponds to an increase in thickness of the double layer κ^{-1}.

A good example is the coupling of oleates (that are often used to liquefy ceramic slurries) at Al_20_3 surfaces, which is to be seen from Fig. 4.2.1.3.4.

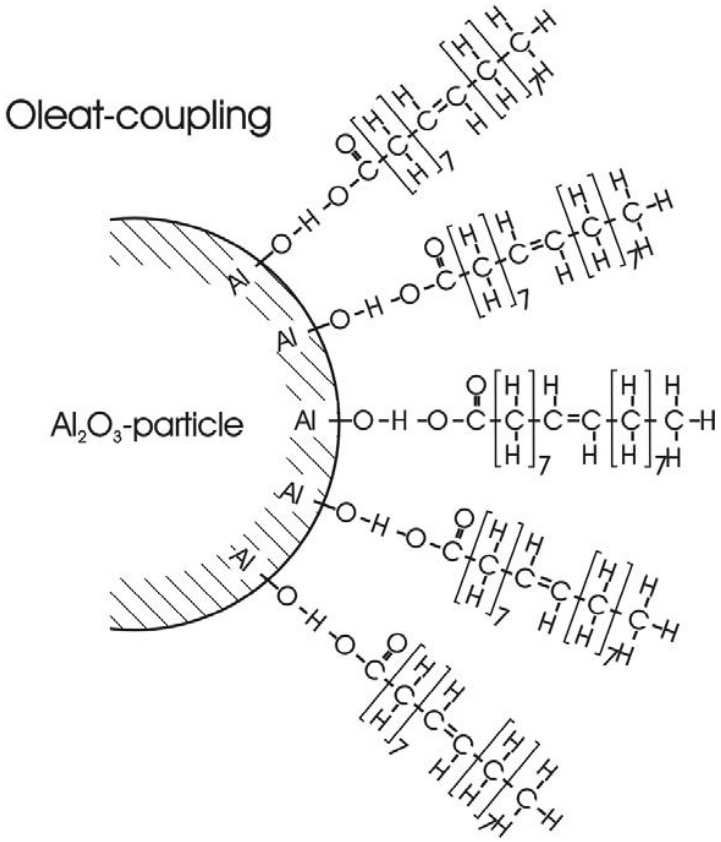

Fig. 4.2.1.3.4: Oleat coupling to a Al_2O_3 surface (schematic).

Fig. 4.2.1.3.5 shows some dispersing agents often used in ceramic suspensions which may couple to powder particle surfaces in a similar way.

Videoclip: Coagulation

Inorganic dispersing agents X=Na, K, NH_4

Polysilicates

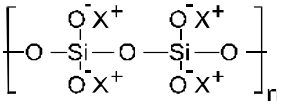

Polyphosphates

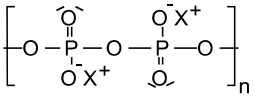

Also used: sodium hydroxide, soda

Organic dispersing agents X=Na, K, NH_4; $R=C_kH_{2k+1}$ mit k=0,1,2,3,...

Polycarbonates

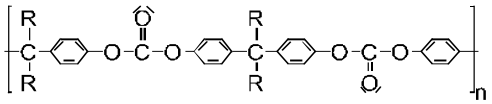

Polyacrylates (*k=0*) and methacrylates (*k=1,2,3,...*)

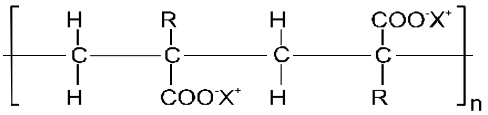

Oxalates

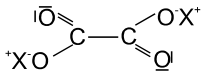

Citrates

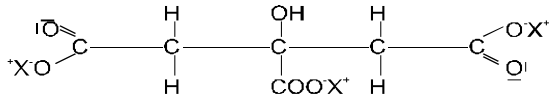

Alcanolamines (Aminoalcohols)

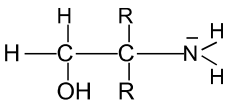

Also used: Tartrates, phosphonates, styrolene maleics acid copolymerisates, cellulosics, ligno sulfonates.

Fig. 4.2.1.3.5: Dispersing agents for ceramic suspensions.

4.2.1.4 Rheological properties of ceramic suspensions

The knowledge of the rheological properties of ceramic suspensions is of essential importance for their preparation. To know how these slurries react against relatively weak outer forces allows understanding the structure of the suspension and the processing characteristics required.

In order to adjust laminar flow in a liquid it is necessary to apply a shear stress. Starting from a stationary layer (i.e. the wall of a slip pipe) a velocity gradient dv/dy (Fig. 4.2.1.4.1) will build up in the liquid when such a stress (for example pump pressure in a slip pipe) is applied.

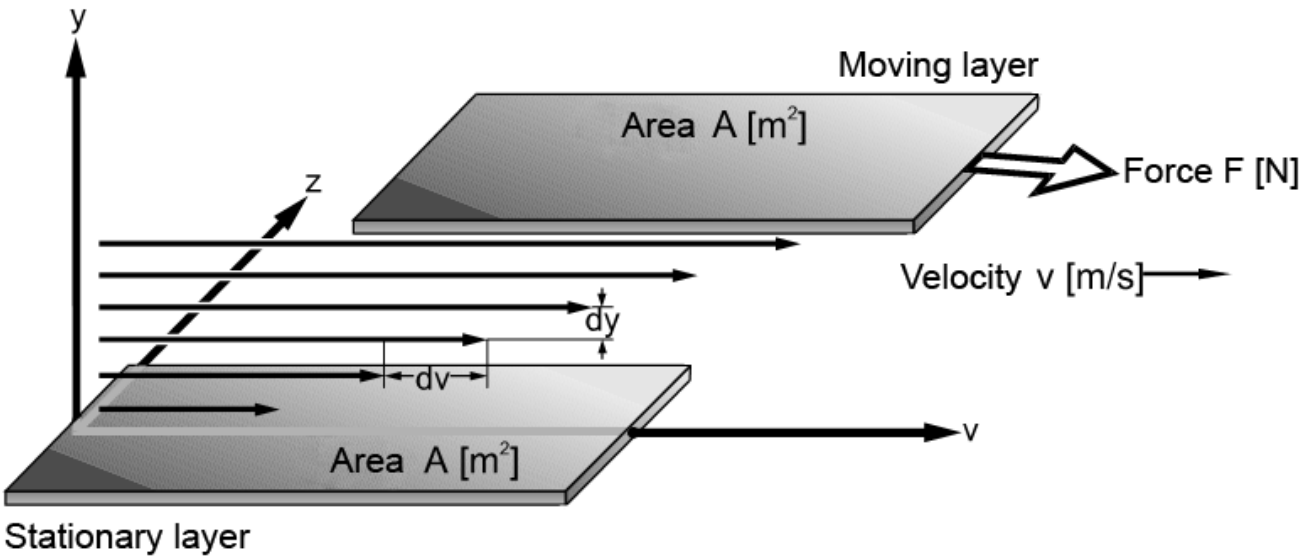

$$\text{Shear stress} \quad \tau = \frac{F}{A} \ [\text{Pa}]$$

$$\text{Shear rate} \quad D = \frac{dv}{dy} \ [\text{s}^{-1}]$$

$$\text{Viscosity} \quad \eta = \frac{\tau}{D} \ [\text{Pa·s}]$$

Fig. 4.2.1.4.1: Model of the viscous flow in a liquid and definition of shear stress, shear rate and coefficient of viscosity.

The velocity of the suspension is 0 at the wall of the slip pipe while it is at its maximum in the middle of the pipe. The size of the shear rate depends on the shear stress and on the material based proportionality factor viscosity η.

$$\frac{dv}{dy} = D = \frac{\tau}{\eta} \quad .$$

The viscosity is a measure for the internal friction of liquid molecules counteracting the flow of the liquid. If there is a linear relation between shear rate and shear stress we talk about Newton‘s liquids (fig. 4.2.1.4.2).

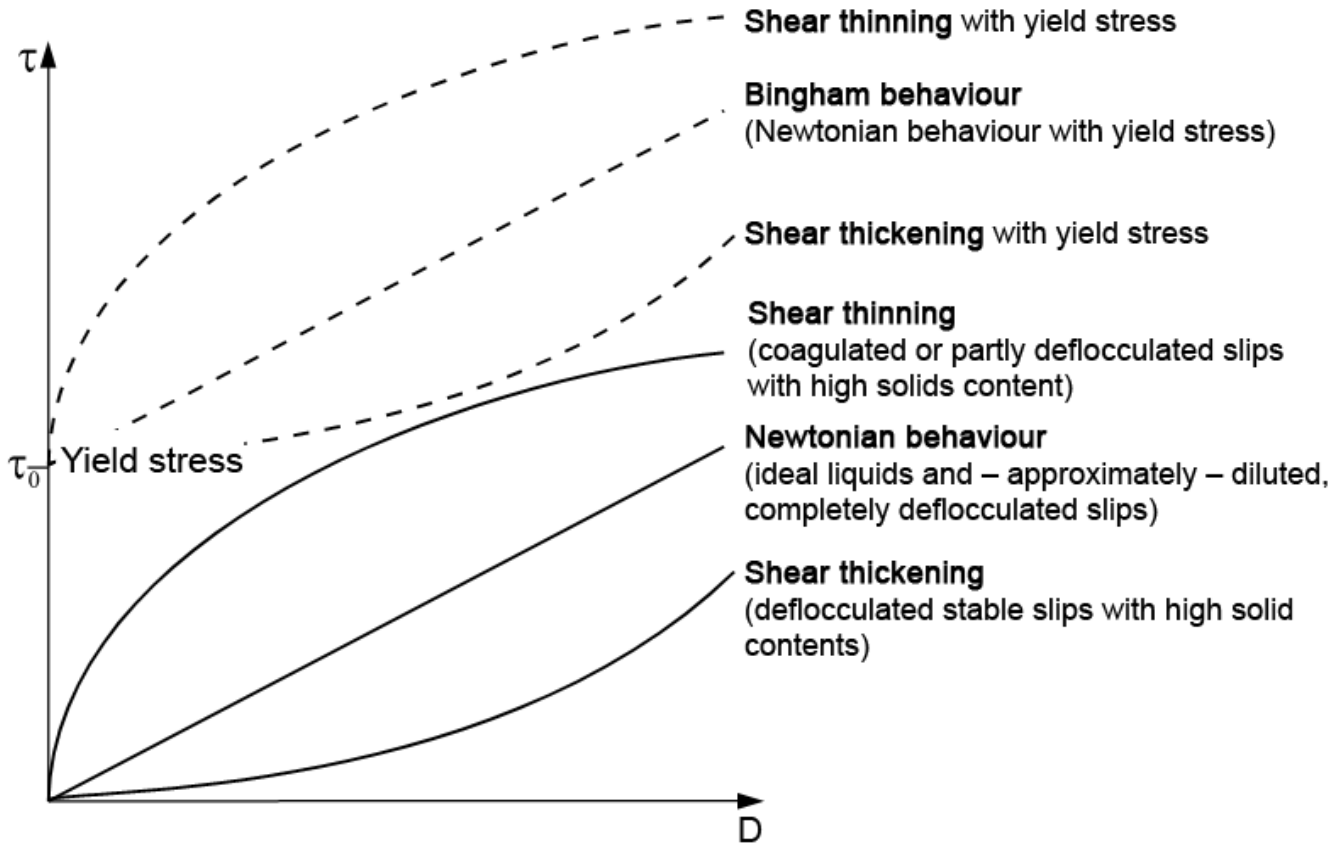

Fig. 4.2.1.4.2: *Variation of s*hear stress with shear rate for different flow behaviour (schematic).

If there are large molecules contained in liquids or when suspensions contain lamellar particles which repulse each other (i.e. kaolin particles) they can direct themselves in a laminar flowing liquid. In addition, in coagulated slurries with high solid yield agglomerates may be destroyed when the shear stress increases. Both appearances reduce the flow resistance and the shear stress required to increase the shear rate by a certain amount will decrease. This behaviour is called shear thinning and may be described mathematically by the below mentioned empiric potential law

$$D = \frac{1}{\eta} \tau^n \quad .$$

η is the apparent viscosity to change with increasing shear strain. In case of shear thinning n will be < 1. n > 1 describes stable slurries with high solid yield where the interaction between the particles and also the apparent viscosity increases with increasing shear strain. This behaviour is called shear thickening.

In suspensions where molecules or particles build up super structures by mutual interactions (i.e. hydrogen bonds or electrostatic effects) they must be destroyed before starting the flow processes which is achieved at the yield stress τ_o. This so-called Bingham behaviour may be described by

$$\tau = \tau_o + \eta \frac{dv}{dy}$$

The dependence on time of the rheological properties is of great practical importance. So for example shear thinning slurries show frequently a decrease in shear stress with time at constant shear rate. In other words the viscosity of the slip (slope of the curves in fig. 4.2.1.4.3) will decrease at constant shear rate with time, the slip becomes more fluid. This thixotropic behaviour is often observed for shear thinning suspensions, where super structures are decomposed in the course of time. This appearance is reversible, as a rule. But in case of a thixotropic slip with yield stress also this value increases sometimes when the slip was kept in neutral position because of further super structures that had been built up.

Some materials show an increase in shear stress at constant shear rate with time i.e. the slip becomes more viscous with increasing time (Fig. 4.2.1.4.3).

This rather rare behaviour is called rheopectic and is observed when due to the slip movement additional bonds between molecules and particles become possible.

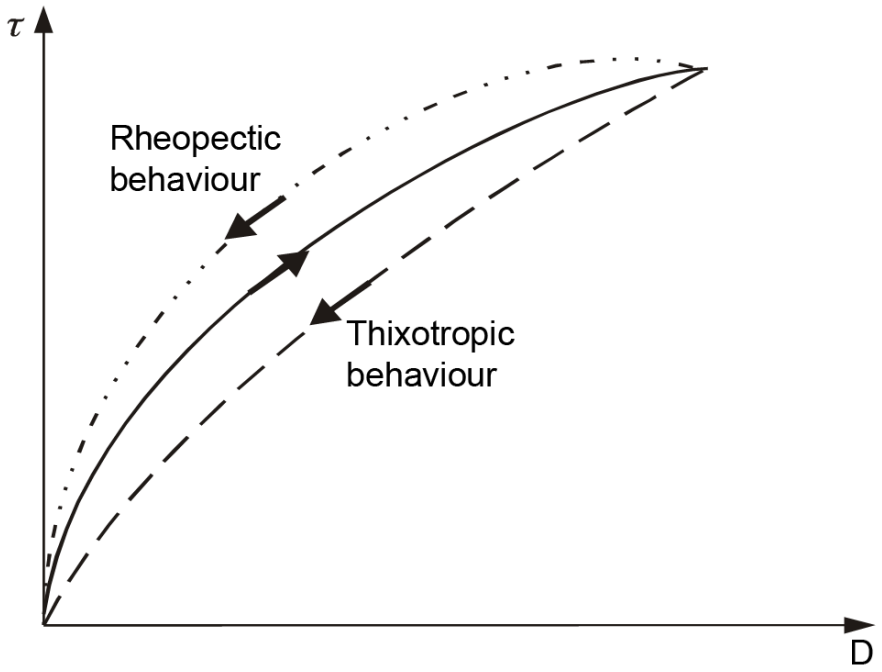

Fig. 4.2.1.4.3: Thixotropic and rheopectic behaviour of ceramic suspensions.

The addition of organic additives (binders, deflocculants) to ceramic suspensions may considerably change the flow curves. Due to the complicated interactions of the organic additives to each other the slip properties are normally empirically optimized in practical use.

With increasing temperature the viscosity of liquids may be reduced as follows

$$\eta = A \exp\left(\frac{Q}{RT}\right)$$

where A and Q = const. Normally ceramic slurries are processed at room temperature. But small thermal fluctuations may cause enormous changes in processing due to the exponential temperature dependence of the viscosity. Moreover, temperatures of 30 to 35°C will very quickly lead to the growth of bacteria cultures that may change the properties of the organic additives considerably and thus the rheological properties of the slurries. This appearance is avoided by adding so-called preservatives.

The viscosity of the suspensions is greater than the viscosity of the liquid. The relation of both to each other is called relative viscosity η_r. For a suspension with particles without any interaction in a Newton's liquid Einstein calculated the viscosity of a laminar flow as follows:

$$\eta_r = \frac{\eta_{Suspension}}{\eta_{Liquid}} = 1 + 2{,}5V_p \quad .$$

where V_p is the share in volume of the dispersed particles. An empiric enlargement for solids concentrations up to 74 vol.% is to be seen from Michaels [11]:

$$\eta = \eta_0 \left(1 + \frac{1{,}25\, V_p}{1 - \frac{V_p}{0{,}74}} \right)^2$$

In practical use the correlations between viscosity and solid yield are much more complex, but in principle the viscosity will increase with increasing solid yield of the suspension.

For processing ceramic slurries great effort is made to set high solid yields (low drying rate!) and to liquefy the slurries in the optimum way. Fig. 4.2.1.4.4 shows the correlation between the zeta potential respectively the formation of a diffuse electric double layer and the viscosity on the example of alumina. Graule et al. [12] determined a viscosity minimum in the acidic and basic range (Fig. 4.2.1.4.4) in Al_2O_3 slurries. This correlates to a characteristic double layer respectively a high zeta potential in these pH ranges (fig. 4.2.1.4.4). In between is a viscosity maximum coinciding with the isoelectric point where the particles develop only low repulsive forces. The optimum double layer is built up by varying the defflocculant concentration and thus the viscosity minimum for the slip preparation is set.

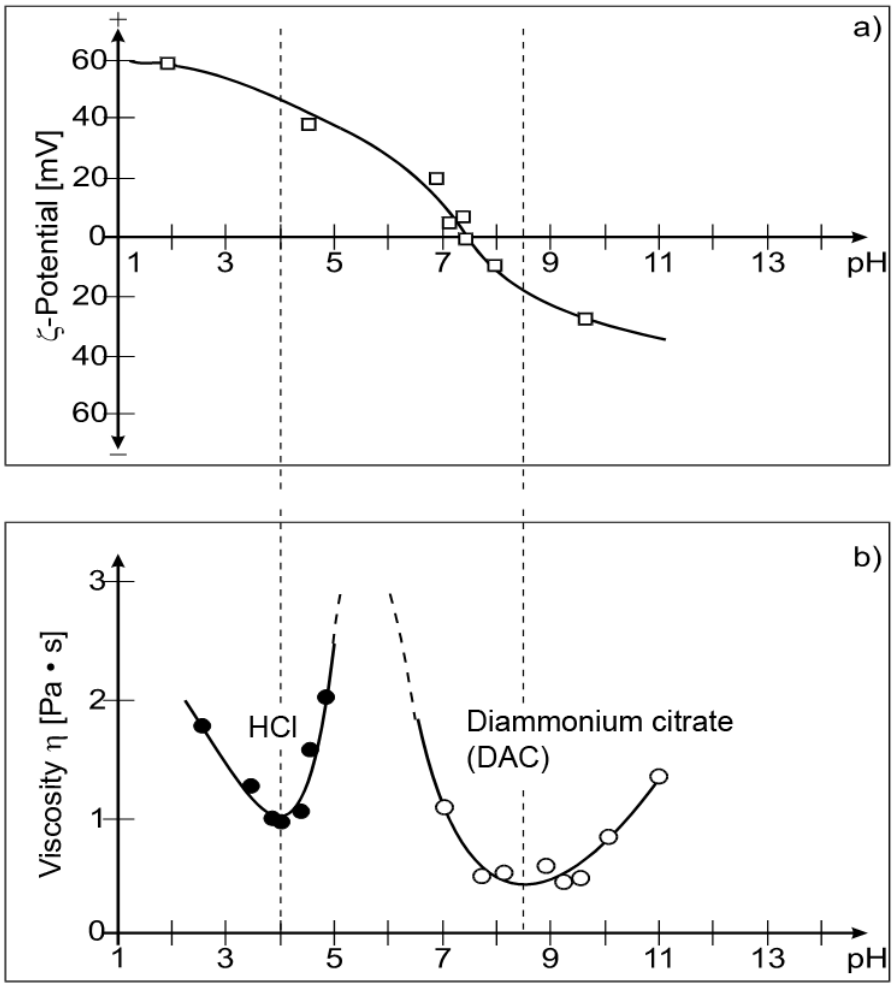

Fig. 4.2.1.4.4: Zeta potential and viscosity of Al_2O_3 suspensions (from [12], [13]).

4.2.2 Plasticity of ceramic systems

Plastic behaviour is normally understood as the plastic deformation of a material by means of dislocation movements, grain boundary sliding and diffusion processes. In the ceramics industry this term has been transferred to heterogeneous material mixtures with a liquid phase that show a permanent deformation after surpassing a yield stress without loosing the unity of the body building particles [14]. That is why we also call it plasticity limited by crack formation for which maximum stresses and deformations may be specified.

Although a lot of trials have been run in order to define and mathematically determine the terms of plasticity respectively ductility, there is no uniform measuring study available up to this date to test this characteristic. The critical point for plasticity evaluation in the main the yield stress, measured as load under definite geometric conditions in the beginning of the forming process and the maximum achievable deformation up to crack formation.

The Pfefferkorn [15] method is still used in many industrial laboratories because of its simplicity. In this test, a disk falls on a cylinder manufactured out of a ceramic feed and the deformation obtained is the measure for the plasticity of the feed. According to Haase [16] in the Pfefferkorn test the kinetic energy of the falling disk is equated with the deformation work done. The yield stress τ_f is calculated from the Pfefferkorn values as follows

$$\tau_f = \frac{m\,H}{2\,V \ln (h_0 / h)}$$

m = mass of the Pfefferkorn disk

H = height of the falling disk

V = volume of the feed cylinder

h_0, h = height of the feed cylinder before and after the compressive strain test

If the Pfefferkorn method is applied by considering the compressive strain until crack formation under slow and quick test conditions and by taking the penetration velocity of a pin under certain conditions as a basis for comparison reasons, you will obtain the plasticity figure according to Dietzel [17] with the respective water content.

In other processes the pressure required to extrude feeds through a die is determined as a function of the yield stress. These methods have been described among others by Macey [18], Linseis [19] and Czerch et al. [20].

The extruded body is characterized by its fracture strength. With increasing water content the fracture strength passes through its maximum while the deformation pressure decreases steadily (Fig. 4.2.2.1). According to Haase [14] the ratio of fracture strength to deformation pressure may be used as a criterion for plasticity, as shown in Fig. 4.2.2.2.

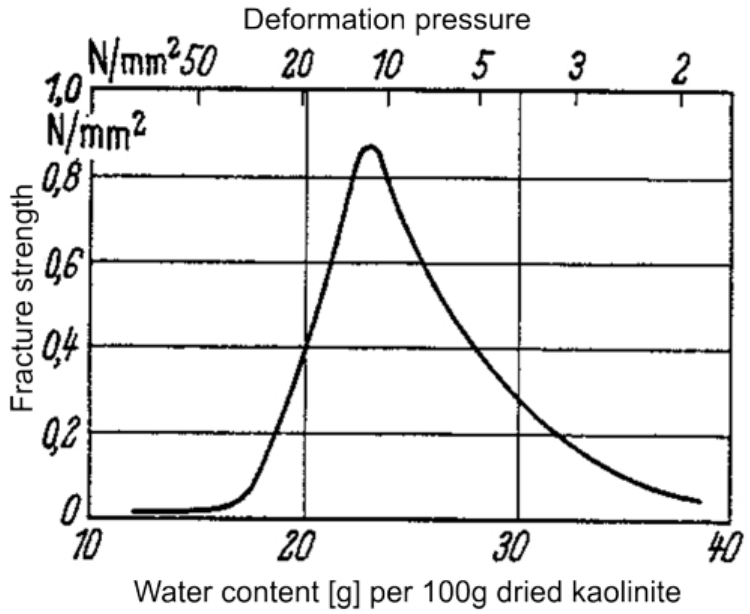

Fig. 4.2.2.1: Dependence of fracture strength and deformation pressure of a Ca kaolinite on the water content according to Czerch et al. [20].

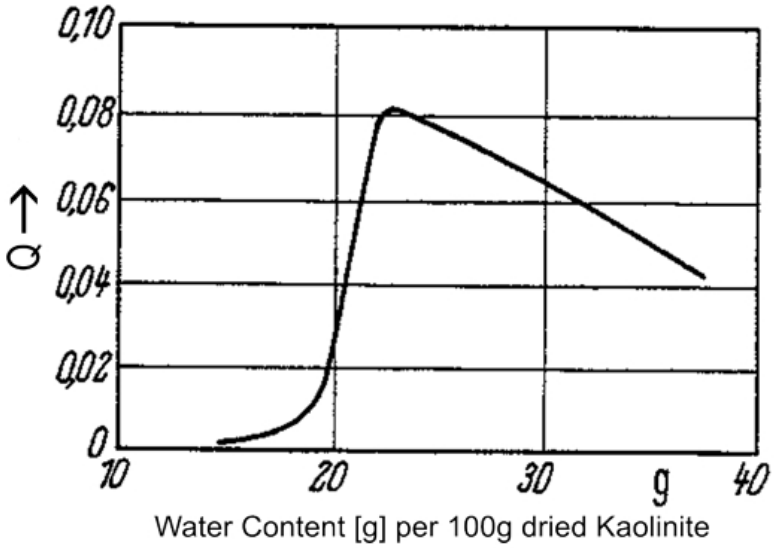

Fig. 4.2.2.2: Evaluation of the curve in Fig. 4.2.2.1 as per the ratio Q = fracture strength /deformation pressure.

Various authors, i.e. Händle [21], determine the characteristic of extrudable clay feeds from the torque of the Brabender equipment for blend preparation under steady water addition. This method is also used for feeds for injection molding whose liquid phase consists of molten thermoplastics.

According to Norton [22] the influence of the water content on the maximum deformation before crack formation may be developed to a function by forming a product with the counter-influence on the yield stress that passes through its maximum at a water content that is characteristic for the feed**.** But also by this method no hint on the suitability for a certain forming process will be obtained, either.

The behaviour of plastic ceramics feeds under a cyclic deformation standard and the observation of the stress-strain curves obtained have been discussed in detail by Astbury, Hennicke, Kersting, Kienow and Kobayashi [23-26]. By these torsional cyclic loading tests, where the torsional stress varies between $+\tau$ and $-\tau$ (in periods of about 1 min.), the elastic and plastic deformation is recorded. The area within the stress-strain hysteresis curves is a measure for the deformation energy that is converted into heat (Fig. 4.2.2.3).

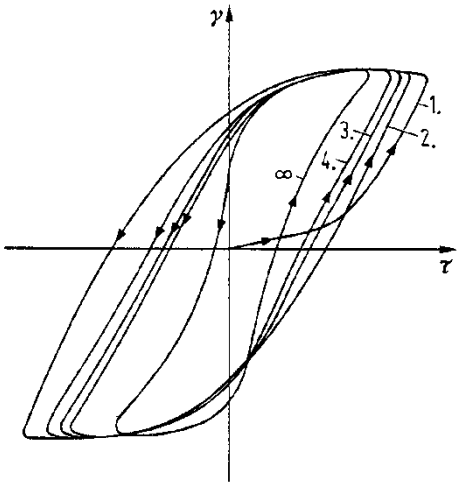

Fig. 4.2.2.3: Stress-strain curves under cyclic torsion tests according to Astbury [23] (only the 1st to the 4th and the equilibrium cycles are shown).

Although the plasticity characteristics are not exactly defined their values of influence will briefly be discussed here.

The plastic behaviour of clay based feeds is determined by the quality and quantity of the liquid phase, the concentration of dissolved salts, the type of solid phases, their particle size distribution and morphology and by the ion concentration on the particles. These correlations are described in detail by Moore/Hennicke [27].

Water has a great adsorption tendency to oxide surfaces and clay minerals. Only 2 mg per gram of kaolin with a specific surface of $13 m^2/g$ are sufficient to obtain a mono-molecular covering and a particle unity by hydrogen bonds. Thicker layers of disoriented liquid water of

more than 10 nm (circa 30 H_2O layers) lead to a mechanical movability of the particles with still efficient residual forces. The fine solids particles may also be unified by the influence of interfacial forces of the water in the small gaps and cavities. In case of still higher water contents the feed becomes liquid, usually showing the non-Newtonian behaviour of shear thinning and an intensified thixotropic appearance. Thus the water content is of great importance for the plasticity of clay minerals and must be optimized for the respective forming process.

With decreasing grain size of the inorganic powder particles both the number of nearest neighbours and the probability of a new adhesion after the deformation increase, so that plasticity will be improved. Platelets (i.e. kaolinite) show a favourable behaviour towards plasticity as they allow sliding over vast areas without loosing their unity [28] when cohering in parallel to each other. According to Mostetzky [29] model observations of water layers between balls or plates show for the latter a lower shear stress to be overcome which explains the positive influence on plasticity.

The ion exchangeability of clay based raw materials leads to a limited bonding of the clay minerals to other solid constituents of the feed like feldspar particles. This bonding capacity increases with decreasing thickness of the platelets. According to Hofmann [30] for montmorillonite with its coating by Na^+ ions this capacity and thus the influence on plasticity may be intensified by swelling up the inner crystalline layers.

If clay based particles are missing in an inorganic powder mixture to make the feed plastic (i.e. in oxide or non-oxide ceramic masses), plasticity can be obtained by adding organic polymers. Such feeds are used for extrusion and injection molding. The additives used, their processability and their function are described in chapters 3.2.2 and 3.2.3.

4.2.3 Granulation

Pressing techniques with powder mixtures being compressed in almost dry condition are preferred for forming ceramic products with appropriate geometries. Ceramic starting powders are normally milled down to the micrometer range in order to increase their sintering capacity. On the other hand, attractive forces arise at the particle surfaces and lead to uncontrolled agglomerations and a bad processability. In order to optimize the flowability and to increase both the bulk density and the storing capability of comminuted powders in silos and hoppers they are granulated before further processing.

4.2.3.1 Production of granules

Spray drying is the most common thermal granulating process in ceramic production. Horizontal fluid bed granulation and spray freeze granulation are also thermal processes but have never approached the importance of spray drying.

Besides fluid bed granulation and compaction the layer agglomeration is quite suited to overtake the spray granulation for economic reasons. That is why this method will be explained here in detail. An explicit survey on the variety of granulating processes is to be seen from Capes [31].

Spray drying

In this thermal granulating process a ceramic slip is atomized to create fine spherical shaped drops which are dried in a hot gas stream. We have to distinguish in the main between rotary and nozzle atomization as they will lead to different distributions of the granule sizes (Fig. 4.2.3.1.1).

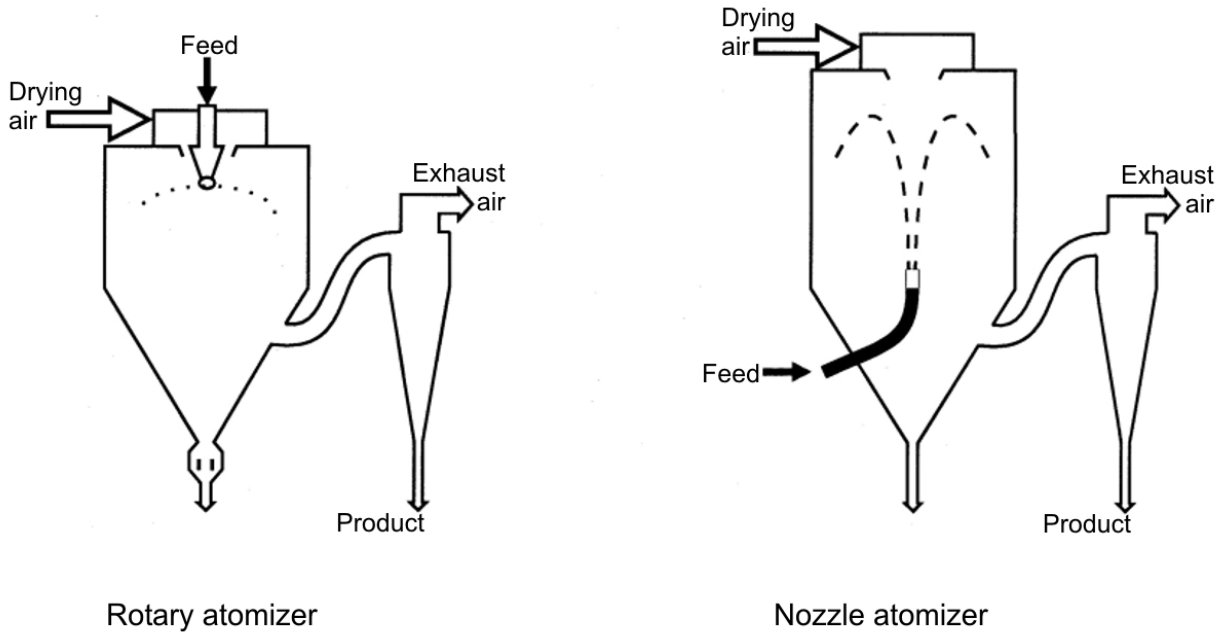

Fig.4.2.3.1.1: Spray driers with different atomizing modes (schematic).

In the case of rotary atomizing the suspension is partitioned into little drops by centrifugal and gravity forces when it leaves a rotating disk. In case of nozzle atomizing different suspensions may be atomized against the hot gas stream through multi-material nozzles. After drying in the hot gas stream, the primary particles are bonded by chemical bridging (Fig. 4.2.3.1.2), by attraction forces between solid particles and by interlocking as described by Rumpf [32, 33]. Due to interfacial and capillary forces of the free liquid surfaces in the chemical bridging, adhesion and cohesion forces in not free moving binder bridges play also a role. Granules present various amounts of liquid between the primary particles (Fig. 4.2.3.1.3) depending on their drying condition. By the free fall of the granules against the hot gas stream in the spray dryer, with a temperature of circa 300°C, the water in the hollow spheres evaporates so that shrinkage and hardening of the granules take place. In order to ensure uniform vapour diffusion from inside the granules to their surface, the temperature and the falling time in the spray dryer must be selected very carefully to avoid both that the granules incrust at their surfaces and that the vapour transport will be hindered.

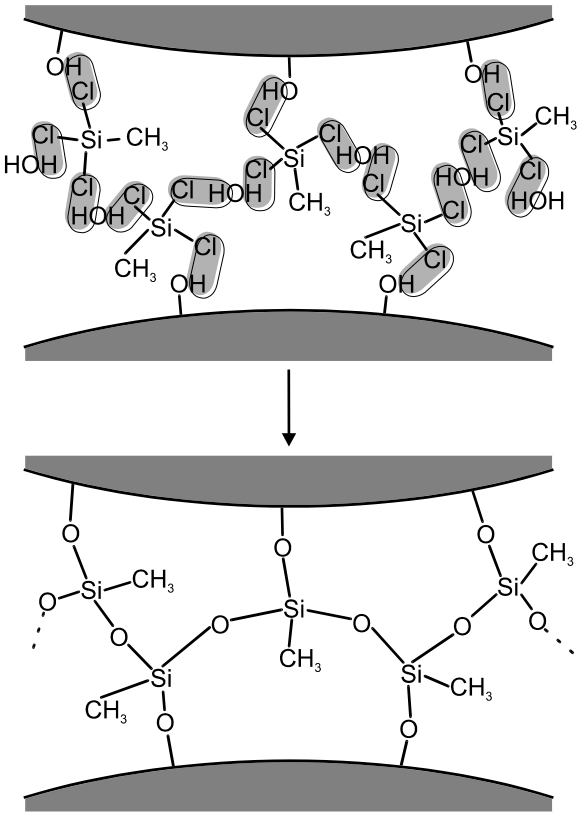

Fig. 4.2.3.1.2: Model of chemical solid-state bridges, due to the presence of Trichlormethylsilane during spray drying [34].

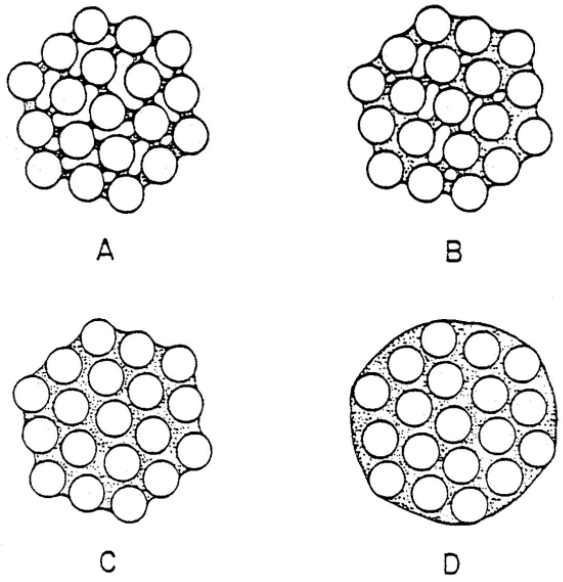

Fig. 4.2.3.1.3: Four stages of agglomerate structures depending on the water content [35].

In order to achieve sufficient green strength after the shaping process, mostly organic binders are added to the suspensions. They enrich at the surfaces on the granules during the drying process, due to their higher evaporation temperatures compared to pure water, so that further transport of water vapour is hindered and a uniform water transport is no longer possible. This leads to cavitation or, in case of high vapour pressure inside the granules, the thin granule wall may burst open (Fig. 4.2.3.1.4). Typical granulate shapes after spray drying are to be seen from Fig. 4.2.3.1.5. The humidity and binder content of the granules will affect their compressibility in the subsequent pressing process and has to be adapted to the respective requirements.

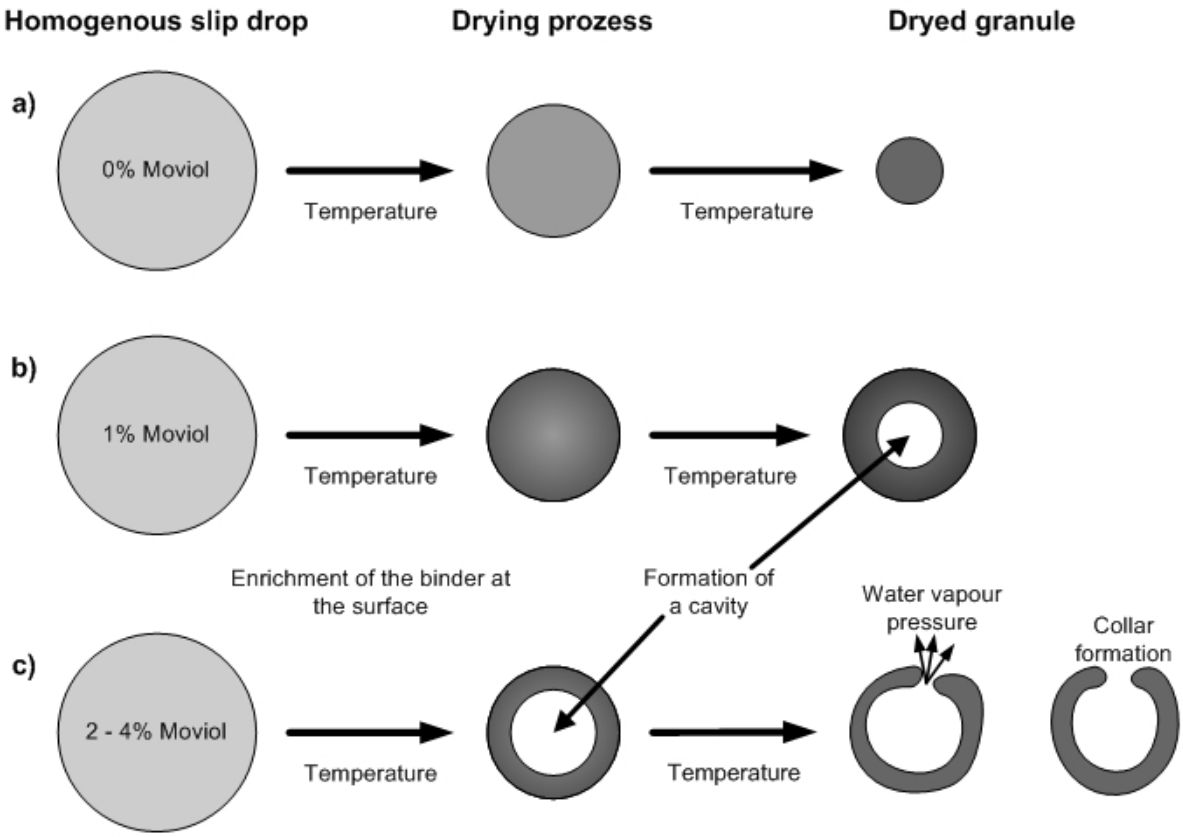

Fig. 4.2.3.1.4: Drying operation in the spray drying process with different binder contents [35] (schematic).

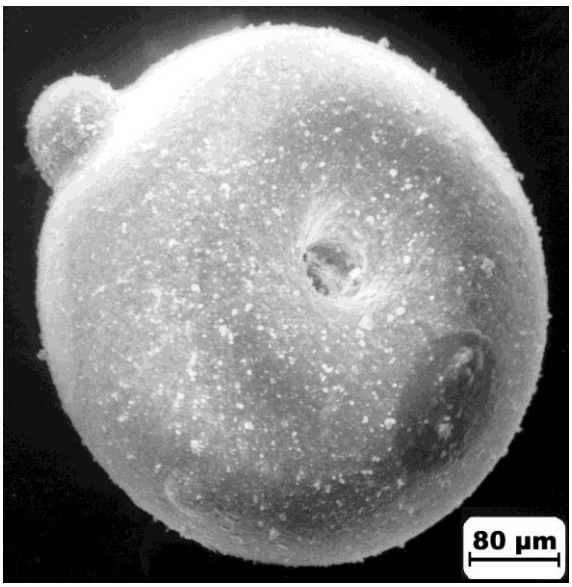

Fig.4.2.3.1.5: Alumina spray granule (SEM).

Videoclip:Granulation by spray drying

Layer agglomeration

In the case of layer agglomeration fine-dispersed powder particles agglomerate to form granules upon addition of water and organic binders while moving in a powder bed. After nucleation, where secondary grains are created by the movement (mixing, stirring, fluid bed etc.) of the powder bed and by simultaneously adding water and after the agglomeration to bigger particles, agglomerates are formed by layer-wise growth of concentric rings (Fig. 4.2.3.1.6).

In the nucleation range, the growth rate of the granules increases considerably and achieves a maximum while forming bigger particles (Fig. 4.2.3.1.6). In [36] the following law is used to describe the growth rate of discontinuous drum granulation:

$$\frac{dD}{dt} = c_1 \, D^3 \exp(c_2 t)$$

c_i = constants
D = diameter of granules
t = time of rotation

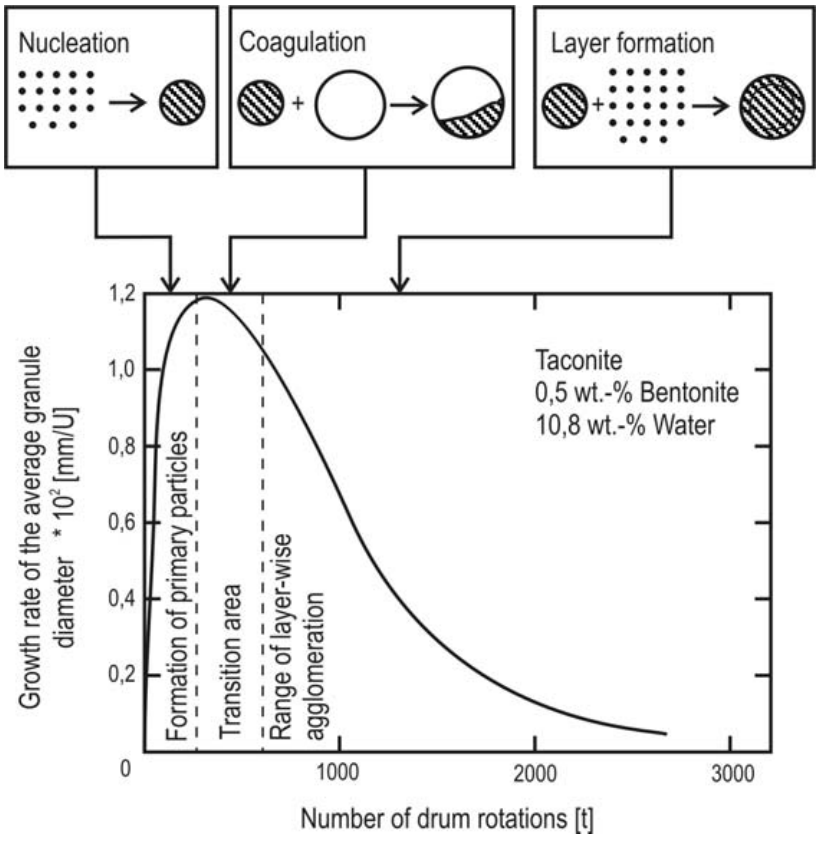

Fig. 4.2.3.1.6: Mechanisms of grain size modification and growth rate of granules at different revolutions of the pelletizing drum [36].

In the range of layerwise agglomeration the growth rate decreases again, the number of primary particles decreases and a further growth can be achieved only by agglomerating small secondary particles. A further movement of the granules may result in destruction by abrasion again.

The layer agglomeration of ceramic materials is done in pelletizing disks, mixers or in a fluid bed as shown in Fig 4.2.3.1.7. In all these processes the particles are moved in relativity to each other and agglomerated by impact, provided that the sticking forces are greater than the always existing separating forces. The agglomeration may be affected by the initial grain size, the temperature, the drum revolution, the gas velocity, the liquid quantity and by the organic binder contents. These values influence the further processability of the granules like it is also the case for the spray granulation process.

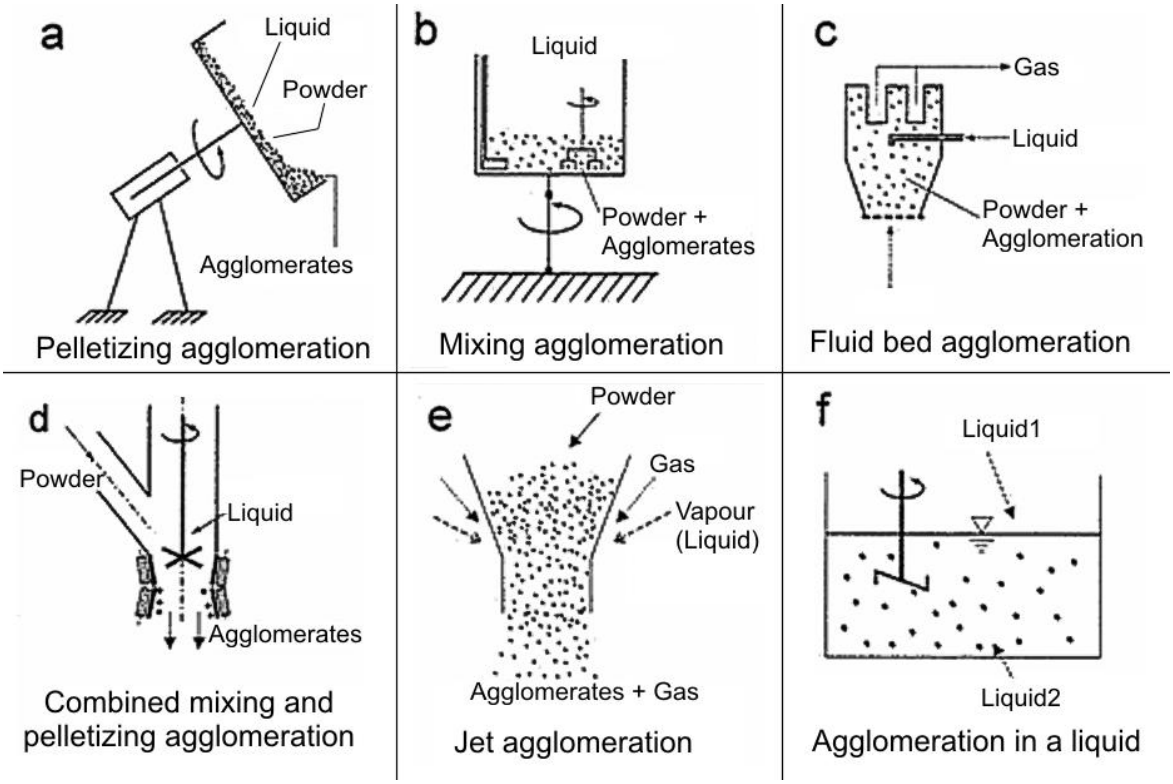

Fig. 4.2.3.1.7: Granulation by layer agglomeration [37].

4.2.3.2 Characterization of granules

Flowability

The two essential characteristics of granulates with regard to their processability are flowability and compressibility. For the filling of pressing molds and the behavior in silos and hoppers, mono-disperse spherical granules with smooth surfaces and high fracture strength would be favourable. Granules consisting of ceramic primary particles, agglomerated by spray drying or layer agglomeration however, have a relatively wide grain size distribution and rough and porous surfaces. Moreover, they contain residual humidity and interfacial active organic additives which affect their flowability. The flowability is often determined by measuring the time required to pour granules out of standardized vessels or by determining the angle of response when pouring out powders. The influence of adhesion forces on the flowability may be better understood when observing a granule rolling over an uneven surface, as described by Frisch et. al. [38], the uneven surface consisting of compressed granules of the same type.

According to fig. 4.2.3.2.1 a granulated grain rolls down if the moment M_I is somewhat greater than M_{II}. Under equilibrium conditions the following applies

$$K_H \cdot r_1 = (K_N + K_A)\, r_2$$

$$\text{resp.} \quad G \sin\alpha\, r_1 = (G \cos\alpha_r + \sigma_A A_A)\, r_2$$

where

K_H = rolling force

K_N = normal force

K_A = adhesion force

σ_A = adhesion stress

G = mass of the granule

α = angle of inclination

r_1 = radius of the granule

A_A = sliding surface

r_2 = radius of the sliding surface

According to Frisch et al.:

$$\sin\alpha = \frac{6 \cdot \sigma_A \sqrt{f^3}}{\rho} \frac{1}{r_2} + \sqrt{f \cos\alpha}$$

where ρ= density of granules and $f = \frac{r_2^2}{4\pi r_1^2}$.

Despite great deviations the relation between sin α and $1/r_1$ can be seen from the results obtained from silicate ceramics granules (Fig. 4.2.3.2.2). For granules with a diameter of 200 µm adhesion stresses were calculated between 0,2 and 0,02 N/mm^2 assuming adhesion forces of 10^{-6} to 10^{-7}N, f-values of 10^{-3} to 10^{-5} and sliding surface radii of 2 to 3,4 µm.

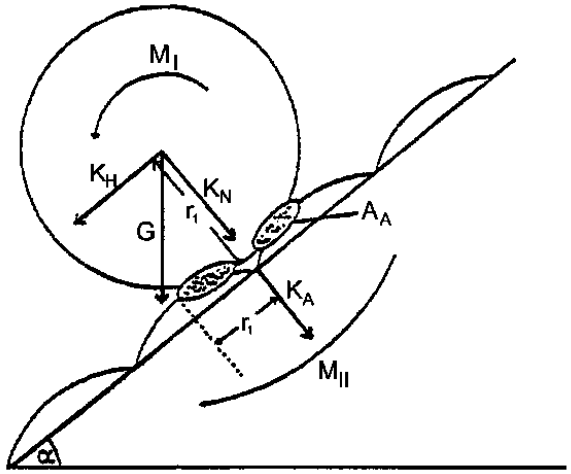

Fig. 4.2.3.2.1: Granule rolling on an uneven surface (explanations see text [38]).

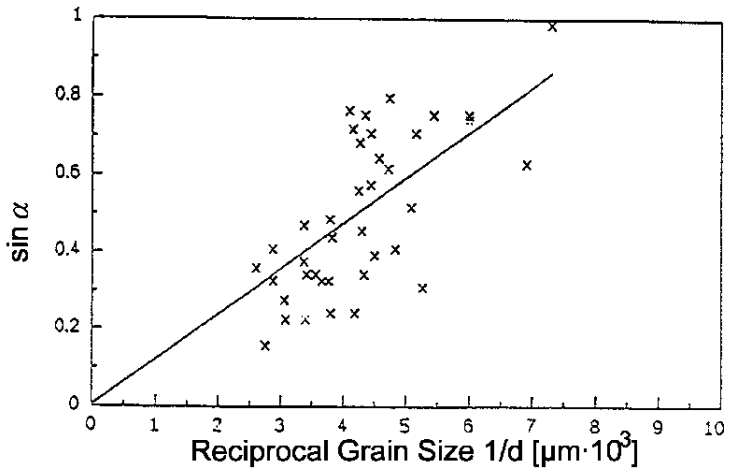

Fig. 4.2.3.2.2: Sinus of the angle of inclination on the surface of a pressed body as a function of the reciprocal grain size of the granules [38].

Strength of individual granules

A further important characteristic of granules both with regard to their flowability and their compressibility is their strength. To determine the strength of individual granules they are fractured between two stamps in a compression test (Fig. 4.2.3.2.3).

Assuming the ideal spherical shape and referring the fracture stress to the meridional area of the sphere [31], the fracture strength of the granule σ_g is calculated as follows [40].

$$\sigma = \frac{4\,F_B}{\pi \cdot d^2}$$

with

F_B = fracture load
d = granule diameter

In practical use the general correlation

$$F_B = \text{const} \cdot d^n$$

is observed with n varying between 1 and 2.

In [31] these variations are related to either the shell formation (n=1) or to the homogeneous distribution of the contact forces between the primary particles over the whole granule cross section (n= 2). That means that variations in the granule structure and size distribution result in a wide strength distribution of the granules. This can lead to problems during pressing and will be discussed in chapter 4.3.3.

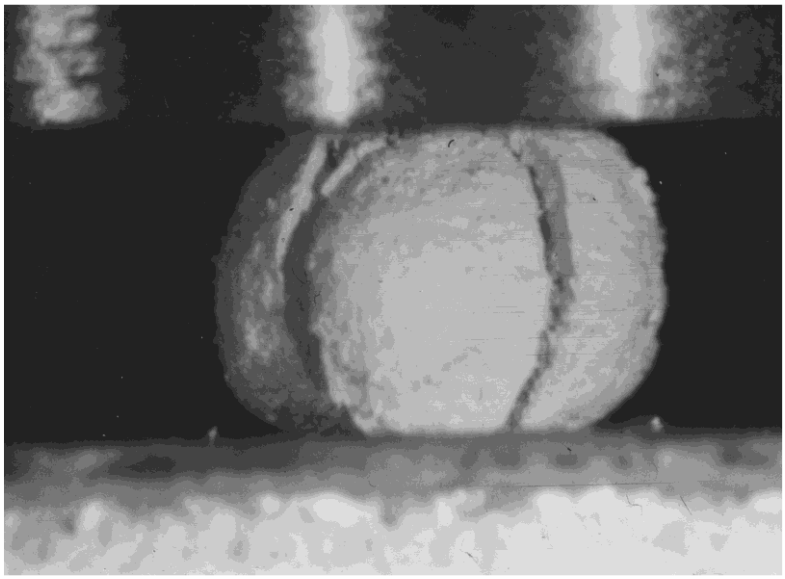

Fig. 4.2.3.2.3: Determination of the strength of individual granules in the pressure test (Courtesy of Dr. Rainer Oberacker, Karlsruhe University [39]).

4.3 Forming

During the forming, deflocculated slurries, plasticized materials or granules are transformed into green bodies with defined size, shape, density and reproducible tolerances. The geometric dimensions required and the quantities to be produced are decisive for determining the forming process to be applied. The shrinkage caused by the subsequent firing process is subject to the fluctuations of the green density and the dimensional tolerances. The reproducibility of these sizes and the avoidance of defects that can hardly be cured any longer in the subsequent sintering decide on the economy of the respective forming process apart from investment and personnel costs. In order to achieve a sufficient green strength for the transport of the parts, but also to optimize the processability characteristics of the initial materials for the respective forming process, organic additives are added to the ceramic feeds to fulfil different functions (Fig. 4.3.1).

Additive	**Function**
Ceramic powder	Matrix
Sintering additive	Densification aid
Solvent	Dispersion
Deflocculant	Control of surface charges and pH, dispersion
Dispersing agent	Deagglomeration
Wetting agent	Reduce of the surface tension of the solvent
Antifoaming agent	Avoidance of bubbles
Preservative	Avoidance of bacteria cultures
Binder	Green strength
Plasticizer	Flexibility
Softener	Flexibility
Lubricant	Reduce die and internal friction, mold release

Fig. 4.3.1: Functions of processing additives in ceramic feeds.